International Journal of Mechanical, Industrial and Aerospace Sciences
ISSN: 2517-9950
Vol:13, No:5, 2019

Study of the Effect of the Contra-Rotating Component on the Performance of the Centrifugal Compressor

Van Thang Nguyen, Amelie Danlos, Richard Paridaens, Farid Bakir

***Abstract*—**This article presents a study of the effect of a contra-rotating component on the efficiency of centrifugal compressors. A contra-rotating centrifugal compressor (CRCC) is constructed using two independent rotors, rotating in the opposite direction and replacing the single rotor of a conventional centrifugal compressor (REF). To respect the geometrical parameters of the REF one, two rotors of the CRCC are designed, based on a single rotor geometry, using the hub and shroud length ratio parameter of the meridional contour. Firstly, the first rotor is designed by choosing a value of length ratio. Then, the second rotor is calculated to be adapted to the fluid flow of the first rotor according aerodynamics principles. In this study, four values of length ratios 0.3, 0.4, 0.5, and 0.6 are used to create four configurations CF1, CF2, CF3, and CF4 respectively. For comparison purpose, the circumferential velocity at the outlet of the REF and the CRCC are preserved, which means that the single rotor of the REF and the second rotor of the CRCC rotate with the same speed of 16000rpm. The speed of the first rotor in this case is chosen to be equal to the speed of the second rotor. The CFD simulation is conducted to compare the performance of the CRCC and the REF with the same boundary conditions. The results show that the configuration with a higher length ratio gives higher pressure rise. However, its efficiency is lower. An investigation over the entire operating range shows that the CF1 is the best configuration in this case. In addition, the CRCC can improve the pressure rise as well as the efficiency by changing the speed of each rotor independently. The results of changing the first rotor speed show with a 130% speed increase, the pressure ratio rises of 8.7% while the efficiency remains stable at the flow rate of the design operating point.

***Keywords*—**Centrifugal compressor, contra-rotating, interaction rotor, vacuum.

I. Introduction

THE contra-rotating component has been applied in turbomachine since 20th century in order to reduce the size, the weight as well as getting higher performances. This component consists of two rotors, which can rotate in inverse directions, with independent speeds. Several studies conducted on contra rotating component proved that using the contra-rotating components can be advantageous in turbo-machineries. Young (1952) [1] and Wilcox (1952) [2] utilized a contra-rotating configuration for axial-flow fan; the results demonstrated that using a contra-rotating fan stage provides higher pressure rise and through-flow capacity. Sharma et al. (1996) [3], [4] conducted a study on the behavior of a contra-rotating axial compressor stage. These authors investigated the dependence of speed ratio on the contra-rotating stage. The results showed that the stalling behavior of a contra-rotating axial compressor stage depends on the speed ratio between the two rotors. If the rotational speed of the second rotor is 50% faster than the first rotor then the stall free range can be improved. However, if the first rotor rotates 50% faster than another one, it leads to increase the load on the first rotor and thus the stall appears earlier in the second rotor. They established that the optimal speed ratio is 0.66:1; the stall will be shifted to a lower flow coefficient. Furukawa et al. (2007) [5] presented an experimental study on performances and flow of contra-rotating pump by combining a rotor-stator and a front-rear rotor. The results show that using a contra rotating component can achieve more compact and lower rotational speed rotor design. In addition, the operating range becomes wider with higher performances by controlling the rotational speed of front and rear rotors individually. Besides, if the front and rear rotors rotate with the same speed, the relative velocity at the rear rotor inlet become higher. However, cavitation occurs at the leading edge of rear rotor due to higher relative velocity so that the design under the condition of $N_{front} > N_{rear}$ was suggested to reduce cavitation. Fukutomi et al. (2008) [6] have used contra-rotating rotors in Sirocco fan to obtain the higher pressure and to make the structure more compact. This work illustrates that the pressure coefficient of contra-rotating fan was 2.5 times as great as the conventional fan because of the increase of the circumferential component of the velocity at the outlet of the second rotor. However, the maximum efficiency of contra-rotating fan is 27% lower than that one. The work of Moroz et al. (2009) [7] in 4-stages and 6-stages axial turbines showed that using the contra-rotating components with the same number of stages can reduce the axial length of 4 stages turbine by 30%, while the performances do not change. In addition, the 6-stages can improve the performances by 0.7% in comparison with the initial turbine. In 2013, Nouri et al. [8] conducted experiments on a contra-rotating axial fan. They showed that using these components could increase the pressure and the efficiency of the axial fan as well as getting wider operating range of mass flow rate. Tosin (2005) [9] showed the results of using contra rotating component for

Van-Thang Nguyen is PhD Student at Dynfluid Laboratory, ENSAM ParisTech, 151 Boulevard de lHopital, 75013 Paris, France (e-mail: Thang.NGUYEN@ ensam.eu).

Amelie Danlos is Associate Professor of the Dynfluid Laboratory, Cnam, 151 Boulevard de l'Hopital, 75013 Paris, France (e-mail: amelie.danlos@lecnam.net).

Richard Paridaens is Researcher of Dynfluid Laboratory, ENSAM ParisTech, 151 Boulevard de l'Hopital, 75013 Paris, France (e-mail: Richard.PARIDAENS@ensam.eu).

Farid Bakir is the Director of the Dynfluid Laboratory, ENSAM ParisTech, 151 Boulevard de l'Hopital, 75013 Paris, France (e-mail: farid.bakir@ensam.eu).

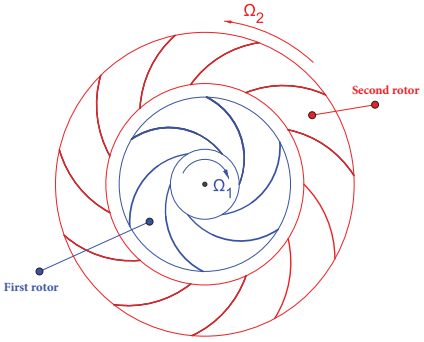

Fig. 1 Diagram of the contra-rotating centrifugal compressor (CRCC) system

Fig. 2 Reference compressor (REF) design

a centrifugal pump. He illustrated that the pump can increase the water column height from 12m to 26m while the efficiency remains constant over 80% by speeding up the first rotor. The literature survey shows that the contra-rotating components can be applied in almost types of turbomachine; however, in our knowledge, there are no study about contra-rotating centrifugal compressor yet. This paper presents a configuration of a contra-rotating centrifugal compressor (CRCC) with a design based on a conventional centrifugal compressor (REF) to analyze the influence of a contra-rotating component on the performance of a centrifugal compressor. In this configuration, CRCC has two rotors: the first upstream rotor rotates at the speed of Ω_1; The second downstream rotor rotates at the speed of Ω_2 in the opposite direction of the first rotor as shown in Fig. 1. The flow out of the first rotor will go directly to the second rotor where the energy is continuously added to the fluid flow to increase the pressure.

II. Rotor Design

A. Reference Compressor

The investigated reference compressor is a centrifugal compressor, which was designed for a vacuum application. The main parameters are presented in Table I.

TABLE I
Parameters of the Reference Compressor (REF)

Parameter	value
D_2	286mm
D_{1h}	59.5mm
D_{1sh}	161mm
β_1	55.7°
β_2	64°
Z	7+7
Q_v	3000 m^3/h
Pressure ratio	1.36
N	16000rpm
Power	28kW

The rotor of the centrifugal compressor presents 7 long blades and 7 splitters, with small vanless diffuser. The flow out of the rotor passes through the spiral where the kinetic energy of the flow is converted into pressure. Fig. 2 illustrates the geometry of the reference compressor.

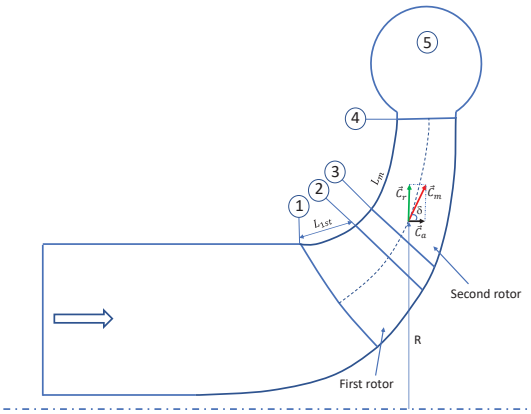

Fig. 3 Meridional contour of the CRCC

B. Design of the CRCC system

The contra-rotating centrifugal compressor is constructed by replacing the single rotor of the REF with two rotors. The same volute is used for both reference compressor and the contra-rotating one. The outlet diameter of first rotor at the upstream is determined by using a length ratio (LR) parameter. This parameter is calculated by the relation (1):

$$LR = \frac{L_{1st}}{L_m} \tag{1}$$

where:
L_{1st} is the length at the hub/shroud contour of the first rotor in meridian plane;
L_m is the total length of the reference rotor in the meridian plane as shown in Fig. 3.

To simplify the calculation process as well as to ensure the rotor compatibility with other components of the compressor, the inlet blade angle of the first rotor and the outlet blade angle of the second rotor remains the same as the ones of the reference rotor.

In order to design the first rotor, firstly the LR is selected to determine the outlet diameter of the first rotor. After that, the outlet blade angle is calculated according to the change of the LR. To do that, the velocity triangle is studied as shown in Fig. 4 to determine the velocity components. The aerodynamic parameters and the velocity component are calculated using

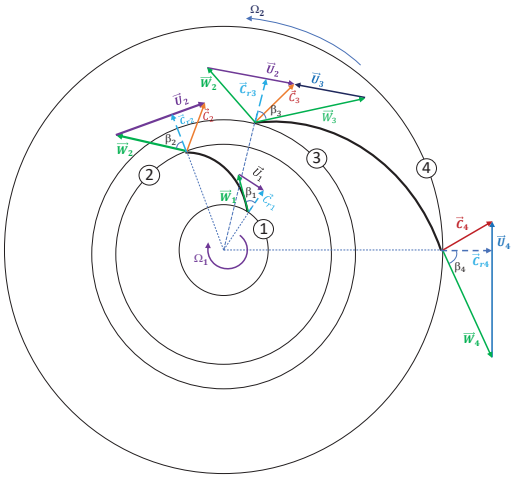

Fig. 4 The velocity triangle applied on the CRCC configuration

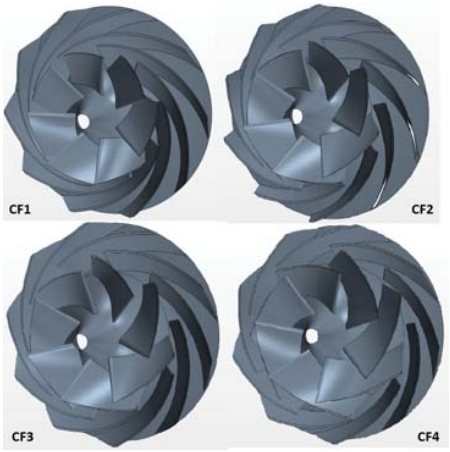

Fig. 5 Four configurations of CRCC system

Table II equations. Finally, the outlet blade angle β_{2b} can be obtained by using (9).

Then, for designing the second rotor, an assumption is used that the input conditions of the second rotor similar to the outlet of the first rotor. The inlet blade angle must be determined and adapted to the flow out of the first rotor by calculating according to the velocity triangle, the blade angle can be determined by using (17).

According to (21), it is easy to see that the total enthalpy rise of the CRCC configuration is higher than the total enthalpy rise of the single rotor because of the reverse rotation effect, which changes the coordinates of the tangential velocity component of the second rotor.

TABLE II
LIST OF EQUATIONS

Parameter	Equation
P_{02}	$P_{02} = P_{01}\left(\frac{T_{02}}{T_{01}}\right)^{\left(\frac{\gamma}{\gamma-1}\right)}$ (2)
T_{02}	$T_{02} = T_{01}\Pi^{\frac{\gamma-1}{\gamma}}$ (3)
ρ_{02}	$\rho_{02} = \frac{P_{02}}{RT_{02}}$ (4)
C_{m2}	$C_{m2} = \frac{\dot{m}}{\rho_{02} S_{02}}$ (5)
C_{r2}	$C_{r2} = C_{m2}\sin\delta$ (6)
σ	$\sigma = \frac{\sqrt{\cos\beta_b}}{Z^{0.7}}$ (7)
β_2	$\tan\beta_2 = \frac{W_{u2}}{C_{m2}}$ (8)
β_{2b}	$\tan\beta_{2b} = \tan\beta_2 + (1-\sigma)\frac{U_2}{C_{m2}}$ (9)
C_{u2}	$C_{u2} = C_p T_1 \frac{\left(\frac{P_2}{P_1}\right)^{\frac{\gamma-1}{\gamma}} - 1}{U_2}$ (10)
W_{u2}	$W_{u2} = U_2 - C_{u2}$ (11)
C_2	$C_2 = \sqrt{C_{u2}^2 + C_{m2}^2}$ (12)
M_2	$M_2 = \frac{C_2}{\sqrt{\gamma RT_{02}}}$ (13)
T_2	$T_2 = \frac{T_{02}}{1+\frac{(\gamma-1)}{2}M_2^2}$ (14)
P_2	$P_2 = \frac{P_{02}}{1+\left(\frac{(\gamma-1)}{2}M_2^2\right)^{\frac{\gamma}{\gamma-1}}}$ (15)
W_{u3}	$W_{u3} = U_3 + C_{u3}$ (16)
β_3	$\tan\beta_3 = \frac{U_3+C_{u2}}{C_{m2}}$ (17)
W_3	$W_3 = \sqrt{W_{u3}^2 + C_{m2}^2}$ (18)
ΔH_1	$\Delta H_1 = U_2 C_{u2} - U_1 C_{u1}$ (19)
ΔH_2	$\Delta H_2 = U_4 C_{u4} + U_3 C_{u3}$ (20)
ΔH_{total}	$\Delta H_{total} = U_4 C_{u4} + U_3 C_{u3} + U_2 C_{u2} - U_1 C_{u1}$ (21)

TABLE III
GEOMETRY PARAMETERS OF FOUR CRCC CONFIGURATIONS

Parameter	CF1	CF2	CF3	CF4
First rotor				
D_{1h}	59.5mm	59.5mm	59.5mm	59.5mm
D_{1sh}	161mm	161mm	161mm	161mm
D_{2h}	118mm	140mm	163mm	186mm
D_{2sh}	176mm	186mm	200.8mm	216mm
β_{1h}	45.25°	45.25°	45.25°	45.25°
β_{1sh}	69.8°	69.8°	69.8°	69.8°
β_{2h}	53.55°	56.77°	60°	65°
β_{2sh}	68.44°	68.87°	69.5°	70°
N_1	16000rpm	16000rpm	16000rpm	16000rpm
Z_1	7	7	7	7
Second rotor				
D_{3h}	59.5mm	59.5mm	59.5mm	59.5mm
D_{3sh}	161mm	161mm	161mm	161mm
D_{4h}	286mm	286mm	286mm	286mm
D_{2sh}	176mm	186mm	200.8mm	216mm
β_{3h}	72.7°	76.06°	78.7°	80.3°
β_{3sh}	76.96°	78.7°	80.27°	81.2°
β_4	64°	64°	64°	64°
N_2	-16000rpm	-16000rpm	-16000rpm	-16000rpm
Z_2	10	10	10	10

C. Geometric Parameters of CRCC Configuration

Four CRCC configurations CF1, CF2, CF3, CF4 are built with four LR values of 0.3, 0.4, 0.5, 0.6 respectively. All configurations have the same number of blades and the rotational speeds. The gap between two rotors is set at 3mm in radial direction. The geometric parameters of four configurations are shown in Table III. Rotors illustrate in Fig. 5.

III. NUMERICAL SIMULATION

The computational fluid dynamic (CFD) simulation is a useful tool to predict the aerodynamic performances of a compressor. The simulation is performed using a three-dimensional, steady state, compressible model with the commercial software Star CCM+. The turbulence model is realizable k-ϵ two-layers and the second order discretization method is selected. The gap between the rotor and the case is not considered in this study. The *flow rate of the design*

operating point (DOP) is given as a boundary condition of the inlet domain at 0.73kg/s. The outlet pressure is imposed at the outlet domain of 101325 Pa. The frozen rotor interface is used between the stationary and the rotational domain. The interface between rotational domains uses mixing-plane method [9], [11]. The mesh convergence is checked to find out the best mesh type and to reduce computational resources. For meshing in Star cmm+ software, the polyhedral and prism layer mesher were used with refined mesh at the blade passage, interface and in the boundary layer. The size of the mesh needs to respect the value of y+ at the wall boundary near to 1. Four types of the mesh were generated by changing of the relative size of the local refined mesh. The number of cells of this mesh is 3.4, 5.26, 8.13 and 11.45 millions respectively.

Fig. 6 shows the mesh convergence of the CRCC and the reference studies. It can be seen that the differential static pressure between the inlet and the outlet of the compressor seems to be stable when the number of cells is higher than 5 million cells. Therefore, it can be concluded that 5 million cells are sufficient to produce grid independent results. The mesh model of two types of compressor are presented in Figs. 7 and 8. Both of the models are meshed with a about 5.26 million cells.

IV. Results and Discussion

To evaluate the performances, the pressure and temperature values are taken from a constant grid surface as mass-average value in the inlet and the outlet domain. The static pressure ratio and the polytropic efficiency are respectively calculated according to the following relations:

$$\Pi = \frac{P_{out}}{P_{in}} \tag{22}$$

$$\eta_p = \frac{\ln\left(\frac{P_{out}}{P_{in}}\right)}{\ln\left(\frac{T_{out}}{T_{in}}\right)} \frac{\gamma - 1}{\gamma} \tag{23}$$

A. Rotor Performance

The rotor performance analysis is conducted to evaluate the impact of contra-rotating component. Fig. 9 illustrates the variation of the static pressure ratio of the contra-rotating components and the reference rotor. It is clear that the contra-rotating system gives a higher pressure ratio than the reference one at the flow rate lower than the DOP. There are three types of tendency: the first type is that the pressure ratio increases when the mass flow rate reduces, after reaching a peak it drops sharply in the CF3 and CF4 configurations. In the second case, the pressure rises rapidly, after reaching the highest value, it becomes almost stable in CF1. While the third one is stable and diminishes at 0.43kg/s in CF2. Looking at the DOP ($\dot{m} = 0.73kg/s$), the pressure ratio increases when the LR of the first rotor rises. The highest pressure ratio can be achieved in the CF4 because of the larger diameter of the outlet first rotor. As a matter of fact, it produces a higher kinetic energy flow into the second rotor. The maximum value of pressure ratio is 1.44 at the mass flow rate 0.43kg/s while it is 1.29 for the reference configuration. The CF1 gives a quite stable at low flow rate and the maximum pressure ratio reaches of 1.34 which increase 5% in comparison with the reference. In contrast, at higher mass flow rate, the pressure ratio of CF1 decreases rapidly because of a smaller inlet surface area of the second rotor.

Fig. 10 presents a variation of the polytropic efficiency of the rotor system at different mass flow rates. Observation shows that the efficiency of the contra-rotating component is always lower than the reference one because of the extra loss at the inlet of the second rotor. Obviously, at low flow rate, the efficiency of the CF1 is always higher than the other ones; the highest efficiency can reach of 78% at the DOP. However, at high flow rate it drops dramatically because of the appearance of the choked region. The lower efficiency of the contra-rotating component can be explained by the high relative Mach number at the leading edge of the second rotor.

Fig. 11 demonstrates the change of the relative Mach number at the leading edge of the second rotor. We can observe that, relative Mach number increases monotonically with the outlet diameter of the first rotor as a results of reverse rotation effect. The high relative Mach number leads to the shock waves and can lead to blockage at the inlet so that it reduces the performances of the rotor.

Concerning the power consumption, Fig. 12 shows that the contra-rotating component needs more energy than the REF because of the higher pressure ratio and the extra loss at the inlet of the second rotor. The CF3 and CF4 have a quite similar power consumption while there is a slight difference between CF1 and CF2. Looking at the mass flow rate of 0.63kg/s, the CF1 and CF2 have the same pressure ratio but the CF2 consumes more energy than that one. It means that this configuration has more loss leading to increase the temperature at the outlet and to reduce the efficiency.

B. Stage Performances

Before analyzing the stage performances of the compressor, the volute performances are tested to estimate the ability of the adaptation between rotor and volute. The volute of the compressor transforms the kinetic energy of the fluid flow from the vanless diffuser or rotor into pressure, with minimum losses. To asset the adaptation of the volute with the contra-rotating rotor, the pressure recovery coefficient and pressure loss coefficient were used. According to [10] the pressure recovery coefficient and the pressure loss coefficient were respectively determined by:

$$C_{pr} = \frac{P_5 - P_4}{P_{04} - P_4} \tag{24}$$

$$\omega = \frac{P_{04} - P_{05}}{P_{04} - P_4} \tag{25}$$

Fig. 13 demonstrates the change of the pressure recovery coefficient of the volute. It is obvious that CF1 and CF2 have a value of C_{pr} close to the reference one while this value for CF3 and CF4 decreases sharply when the mass flow rate increases. Near the surge region, the C_{pr} is positive with all configurations. At the DOP, the value of C_{pr} of CF4 is approximately zero while CF1, CF2 and CF3 remain positive

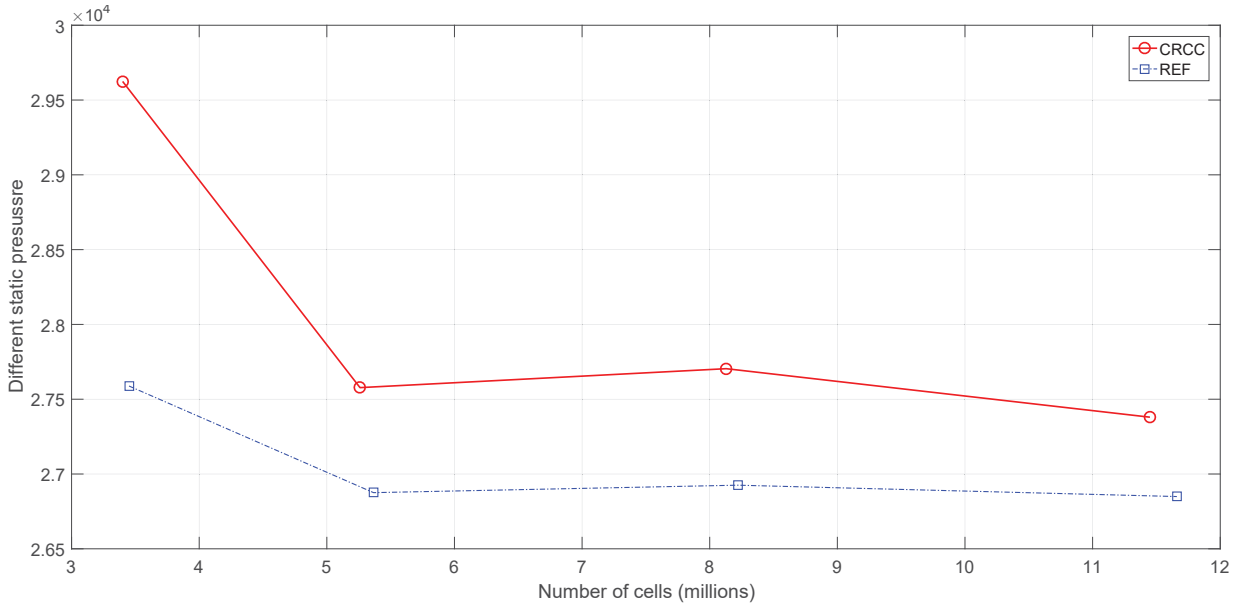

Fig. 6 Study of the mesh sensitivity

Fig. 7 Different views of reference compressor mesh

Fig. 8 Different views of CRCC compressor mesh

about of 0.5 to 0.7. At very high flow rates, C_{pr} of CF3 and CF4 decreases rapidly and becomes negative at -0.6 and -1.5 respectively. Consequently, the CF1,CF2 and CF3 can recover pressure better than CF4.

Fig. 14 illustrates the variation of the loss coefficient with the mass flow rate. It can be seen that, the value of ω remains stable in CF1 and CF2 and approximately equal to the reference one, slightly increases in CF3 and rapidly rises in CF4 when the mass flow rate increases. In general, CF1 and CF2 are well adapted to the volute while CF3 and CF4 configurations present higher pressure loss.

Fig. 15 presents static pressure ratio of the stage of the CRCC according to the mass flow rate variation. It is obvious that, the pressure ratio of the stage of the CRCC is actually improved at a flow rate lower than the DOP. The most important improvement is found for CF1, CF3 and CF4 configurations while CF2 remains stable and close to the reference system. Near surge region, the pressure ratio of CF1, CF3, CF4 have similar values while CF2 has value similar to the reference one. CF1 permits to obtain a pressure ratio more stable than other configurations.

Fig. 16 shows the global polytropic efficiency of the compressor. It is clear that CF1 gives the best efficiency of 80% at the DOP. It reduces 5% in comparison with the reference configuration. Therefore, CF1 will be selected to build the CRCC in a further study.

C. Effect of the Rotor Speed

The advantage of the CRCC is the independency of each rotor rotational speed. Changing the speed of the first rotor or the second rotor can obtain different characteristics of the compressor. In this study, the speed of the first rotor increases while the speed of the second rotor is constant. Three values

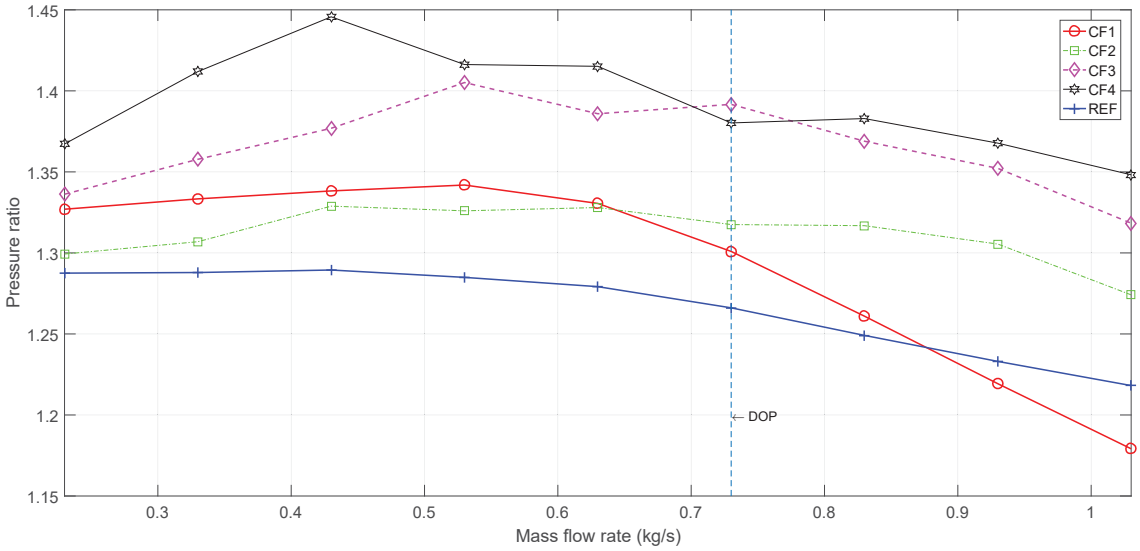

Fig. 9 Pressure ratio (static to static) of rotor

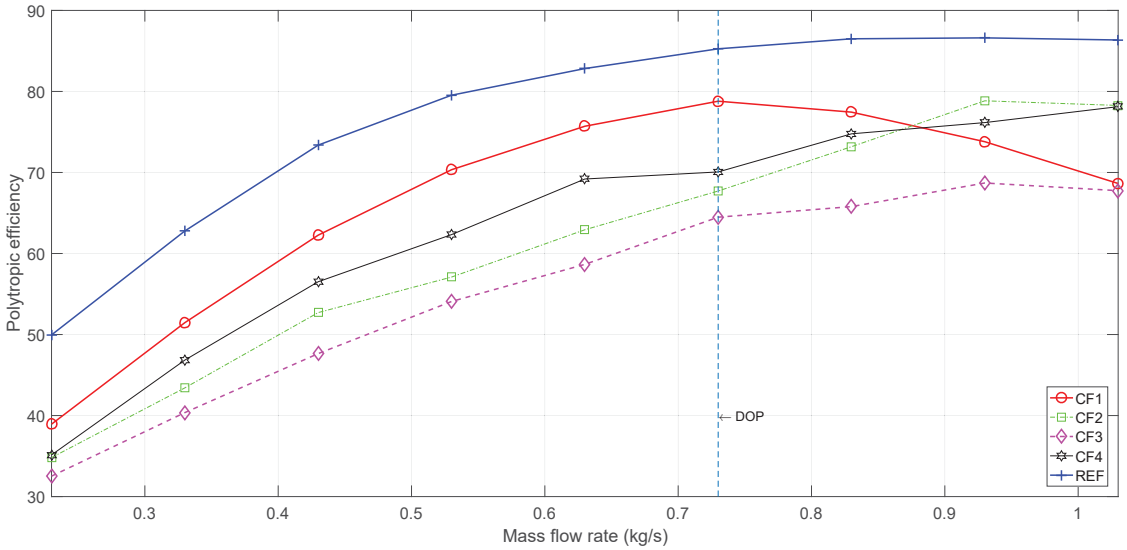

Fig. 10 Polytropic efficiency (static to static) of rotor

of rotational speed of the first rotor were selected: 176000rpm, 19200rpm and 20800rpm corresponding to an increasing speed of 110%, 120% and 130% respectively.

Fig. 17 shows the variation of static pressure ratio when the rotational speed of the first rotor is increased. It is obvious that the static pressure ratio rises with higher rotational speed of the first rotor. At the DOP, when the rotational speed increases 10% we can get the pressure ratio rise about 3%. Consequently, at the speed of 130% speed of the design operating point, the CRCC can increase pressure ratio up to 8.7% in comparison with the reference at the DOP. The maximum pressure ratio of CRCC configuration can reach of 1.53 with the first rotor speed of 130% speed of the design operating point, while the pressure ratio of the REF is 1.41 at a flow rate of 0.43kg/s.

Fig. 18 presents the curve of the efficiency of the CRCC at the different rotational speeds. The polytropic efficiency reaches a peak at the DOP and seems to be constant about 80% when the speed of the first rotor increases. In addition, it is slightly reduced at a flow rate lower than the DOP and is increased at a higher flow rate.

V. Conclusion

The impact of the contra-rotating component on the performances of a centrifugal compressor was carried out.

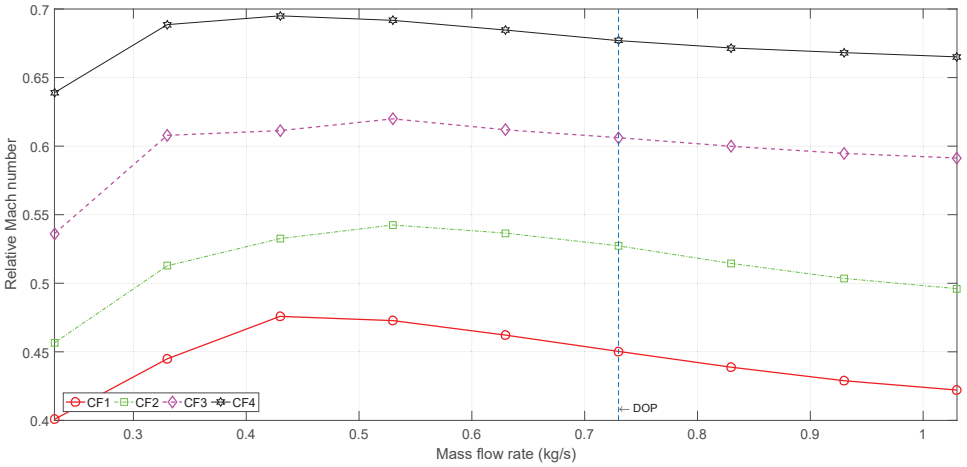

Fig. 11 Relative Mach number at the inlet of the second rotor

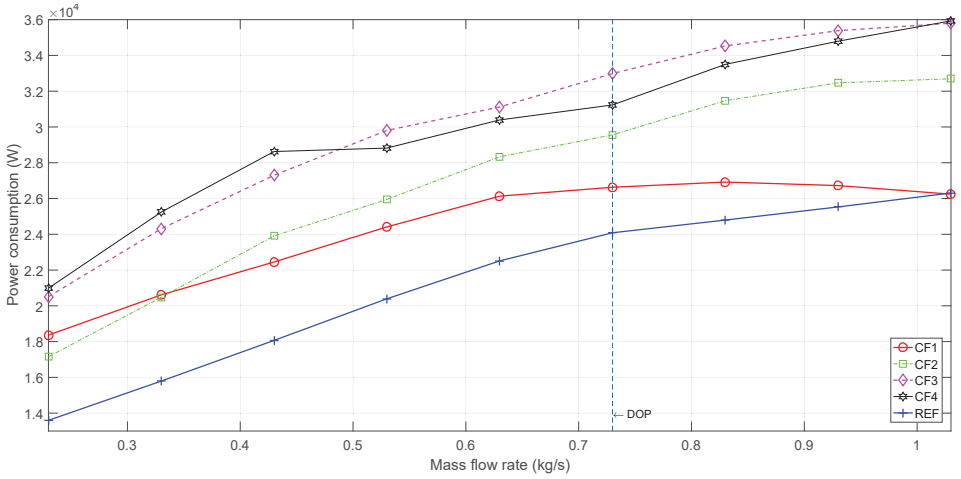

Fig. 12 Power consumption of the different studied configurations

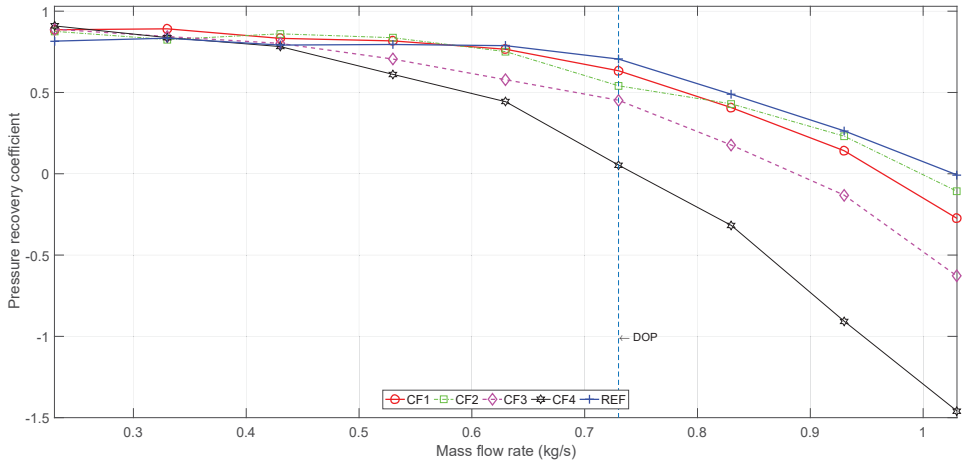

Fig. 13 Pressure recovery coefficient

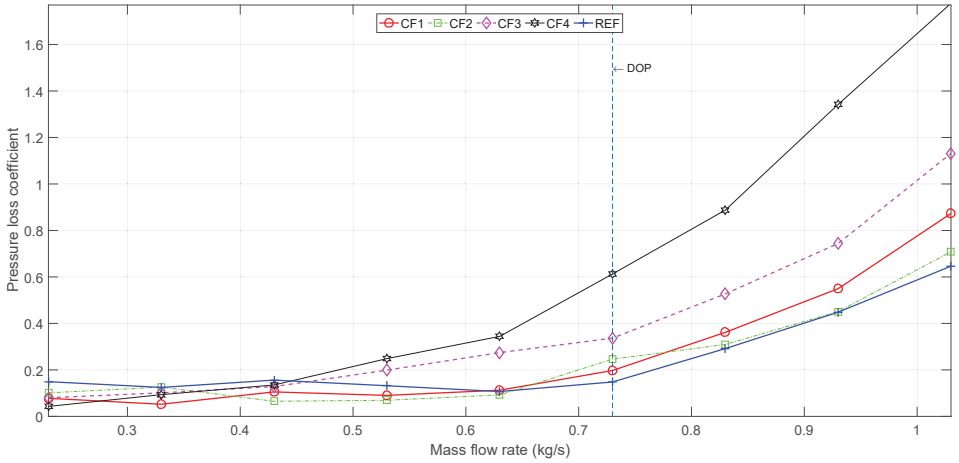

Fig. 14 Pressure loss coefficient

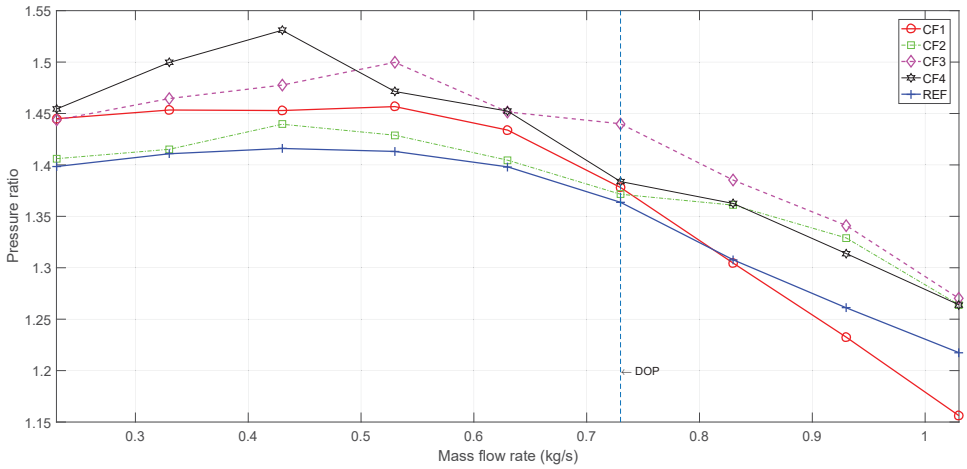

Fig. 15 Pressure ratio of the stage

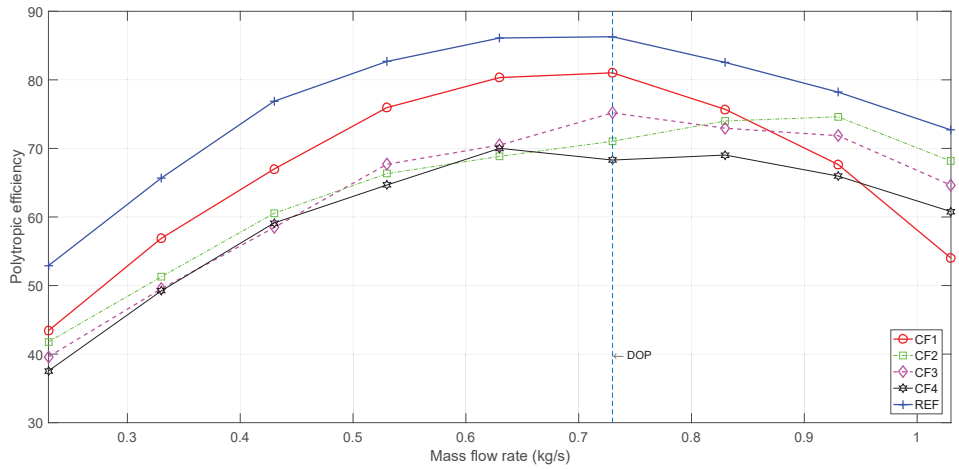

Fig. 16 Polytropic efficicency of the stage

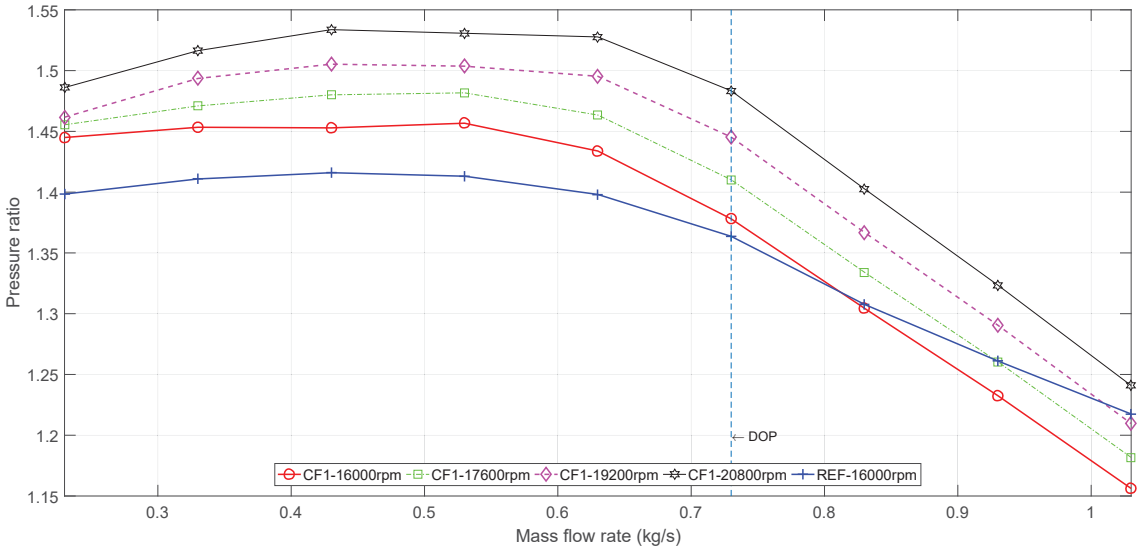

Fig. 17 Pressure ratio (static to static) at different speed of the first rotor

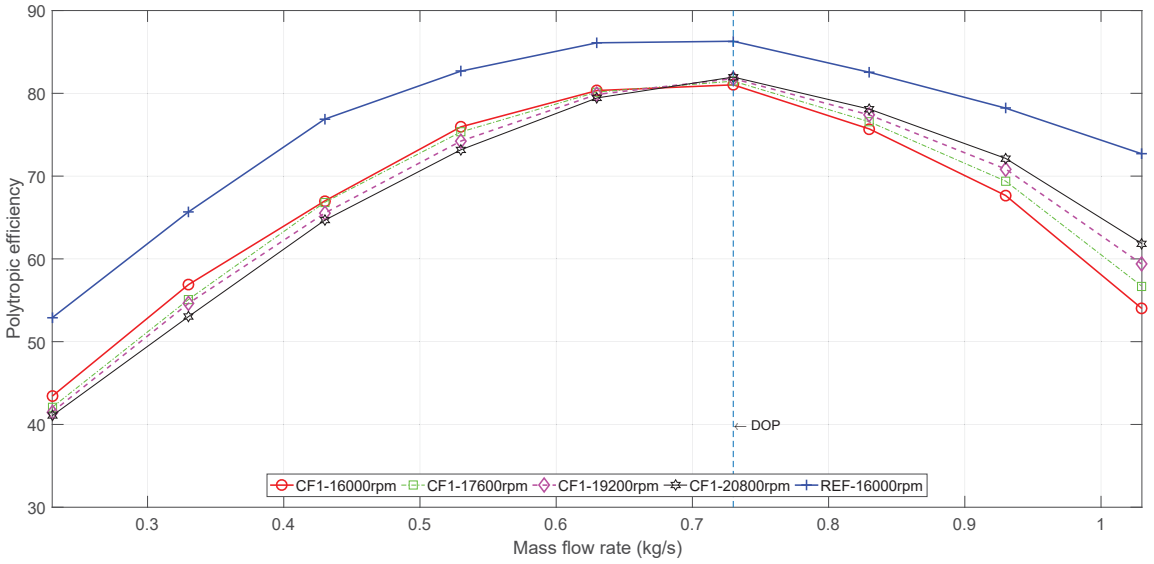

Fig. 18 Polytropic efficiency at different speed of the first rotor

Four configurations of the CRCC were made based on the geometry of the reference rotor. The study shows that:

The contra-rotating component can improve pressure ratio of the compressor. The pressure ratio rise depends on the length ratio of the first rotor. The configuration with a higher length ratio gives more pressure ratio rise, however, the efficiency decreases rapidly.

The CF1 and CF2 configurations are well adapted with the volute of the compressor because of the higher pressure recovery coefficient and the lower pressure loss coefficient. In addition, the efficiency of the CF1 reaches a highest value of 80% at the DOP so that this configuration is selected to build the CRCC for a further study.

The investigation of the variation of the first rotor rotational speed shows that it can improve the pressure ratio up to 8.7% at the DOP with the speed increase of 130% speed of design operating point while the efficiency remains stable.

In a further study, measurements will be conducted on the test bench to observe performances and to study especially the surge region by changing the rotational speed of the rotor. The CRCC may control and improve the appearance of the surge limit of the centrifugal compressor.

Acknowledgment

The authors would like to thank the Vietnam government supported finance and the Internal Flow and Turbomachinery Team at Dynfluid with all support for this study.

NOMENCLATURE

P	Static pressure	[Pa]
P_0	Total pressure	[Pa]
T	Static temperature	[K]
T_0	Total temperature	[K]
C	Absolute velocity	$[m/s]$
C_u	Absolute tangential velocity	$[m/s]$
C_m	Meridional velocity	$[m/s]$
W	Relative velocity	$[m/s]$
W_u	Relative tangential velocity	$[m/s]$
U	Blade velocity	$[m/s]$
M	Mach number	
R	Gas constant	$[J/kgK]$
C_{pr}	Pressure recovery coefficient	
L_{1st}	Meridional length of the first rotor	[m]
L_m	Total meridional length of rotor	[m]
LR	Length ratio	
N	Rotational speed	[rpm]
Z	number of blade	

Greek symbol

β_b	Blade angle	$[^\circ]$
β	Fluid flow angle	$[^\circ]$
δ	Angle between meridional direction and rotational axis	$[^\circ]$
ρ	Density	$[kg/m^3]$
σ	Slip factor	
γ	Specific heat	
Π	Pressure ratio	
η	Efficiency	
ω	Loss coeffiecient	

Subscripts

1	Inlet of the first rotor
2	Outlet of the first rotor
3	Inlet of the second rotor
4	Outlet of the second rotor
5	Outlet of the volute
r	Radial direction
a	Axial direction
m	Meridional direction

Abbreviations

REF	Reference compressor
CRCC	Contra-rotating centrifugal compressor
DOP	Design operating point

REFERENCES

[1] R. H. Young. Counter rotating fans. JHIVE, 18, (1952).
[2] Ward W. Wilcox. An analysis of the potentialities of a two-stage counter-rotating supersonic compressor. (1952).
[3] P. B. Sharma and A. Adekoya. A review of recent research on contra-rotating axial flow compressor stage. In ASME 1996 International Gas Turbine and Aero engine Congress and Exhibition, pages V001T01A073V001T01A073. American Society of Mechanical Engineers, (1996).
[4] P. B. Sharma, Y. P. Jain, N. K. Jha, and B. B. Khanna. Stalling behavior of a contra-rotating axial compressor stage. In International Symposium on Air Breathing Engines, 7th, Beijing, Peoples Republic of China, pages 734740, (1985).
[5] A. Furukawa, T. Shigemitsu, and S. Watanabe. Performance test and flow measurement of contra-rotating axial flow pump. Journal of Thermal Science, 16(1):713, (2007).
[6] J. Fukutomi, T. Shigemitsu, T. Yasunobu. Performance and internal flow of sirofoilcco fan using contra-rotating rotors. Journal of Thermal Science, 17(1), 3541, (2008). https://doi.org/10.1007/s11630-008-0035-8.
[7] L. Moroz, P. Pagur, Y. Govorushchenko and K. Grebennik. Comparison of counter rotating and traditional axial aircraft low-pressure turbines integral and detailed performances. In Int. Symp. On Heat Transfer in Gas Turbine Systems, (2009).
[8] H. Nouri, A. Danlos, F. Ravelet,F. Bakir, C. Sarraf. Experimental Study of the Instationary Flow Between Two Ducted Counter-Rotating Rotors. Journal of Engineering for Gas Turbines and Power, 135(2), 22601, (2013). https://doi.org/10.1115/1.4007756.
[9] S. Tosin, A. Dreiss,J. Friedrichs. Experimental and numerical investigation of a counter-rotating mixed-flow single stage pump. ASME Expo 2015, 111, 2015.
[10] H. Pitknen,H. Esa, P. Sallinen,J. Larjola. CFD Analysis of a Centrifugal Compressor Impeller and Volute. International Gas Turbine Aeroengine Congress Exhibition, (1997), 18. https://doi.org/10.1115/99-GT-436.
[11] C. Robinson,M. Casey,B. Hutchinson,R. Steed. Impeller-Diffuser Interaction In Centrifugal Compressors, 111, (2011).